Cell Swelling Activates ATP-dependent Voltage-gated Chloride Channels in M-1 Mouse Cortical Collecting Duct Cells

KATHRIN MEYER and CHRISTOPH KORBMACHER

From the Zentrum der Physiologie, Klinikum der Johann Wolfgang Goethe-Universität, D-60590 Frankfurt am Main, Germany

ABSTRACT In the present study we used whole-cell patch clamp recordings to investigate swelling-activated Cl^- currents ($I_{Cl\text{-}swell}$) in M-1 mouse cortical collecting duct (CCD) cells. Hypotonic cell swelling reversibly increased the whole-cell Cl^- conductance by about 30-fold. The *I-V* relationship was outwardly-rectifying and $I_{Cl\text{-}swell}$ displayed a characteristic voltage-dependence with relatively fast inactivation upon large depolarizing and slow activation upon hyperpolarizing voltage steps. Reversal potential measurements revealed a selectivity sequence $SCN^- > I^- > Br^- > Cl^- > >$ gluconate. $I_{Cl\text{-}swell}$ was inhibited by tamoxifen, NPPB (5-nitro-2(3-phenylpropylamino)-benzoate), DIDS (4,4′-diisothiocyanostilbene-2,2′-disulphonic acid), flufenamic acid, niflumic acid, and glibenclamide, in descending order of potency. Extracellular cAMP had no significant effect. $I_{Cl\text{-}swell}$ was Ca^{2+} independent, but current activation depended on the presence of a high-energy γ-phosphate group from intracellular ATP or ATPγS. Moreover, it depended on the presence of intracellular Mg^{2+} and was inhibited by staurosporine, which indicates that a phosphorylation step is involved in channel activation. Increasing the cytosolic Ca^{2+} concentration by using ionomycin stimulated Cl^- currents with a voltage dependence different from that of $I_{Cl\text{-}swell}$. Analysis of whole-cell current records during early onset of $I_{Cl\text{-}swell}$ and during final recovery revealed discontinuous step-like changes of the whole-cell current level which were not observed under nonswelling conditions. A single-channel *I-V* curve was constructed using the smallest resolvable current transitions detected at various holding potentials and revealed a slope conductance of 55, 15, and 8 pS at +120, 0, and −120 mV, respectively. The larger current steps observed in these recordings had about 2, 3, or 4 times the size of the putative single-channel current amplitude, suggesting a coordinated gating of several individual channels or channel subunits. In conclusion we have functionally characterized $I_{Cl\text{-}swell}$ in M-1 CCD cells and have identified the underlying single channels in whole-cell current recordings. Key words: volume regulation • hypotonic cell swelling • renal epithelial cells • ion channels • patch clamp

INTRODUCTION

Cell-volume regulation mechanisms have been studied in many different cell types (for review, see Lang et al., 1993). To avoid excessive cell swelling in response to extracellular hypotonicity, most cells activate conductances for K^+ and Cl^-. The resulting KCl efflux reduces cellular osmolyte content and thereby inverts the osmotic gradient and the direction of H_2O flow. Over the past few years intensive research efforts have been aimed at identifying the underlying swelling-activated ion channels and at elucidating their mechanism of activation. In particular swelling-activated Cl^- channels have been studied in a variety of cell types using electrophysiological techniques and molecular biological approaches. Cells may possess several different types of volume-sensitive anion channels that may have different volume regulatory functions (for review, see Strange et al. 1996). The single-channel properties of these swelling-activated Cl^- channels and their molecular identity are poorly understood despite their widespread occurrence. Several putative Cl^- channel proteins have been cloned (for review, see Pusch and Jentsch, 1994). However, at present it is not yet clear how many functionally distinct types of swelling-activated Cl^- channels exist and how the endogenously expressed channels are related to the cloned proteins, which belong to several different gene families.

Collecting duct cells in vivo are exposed to a wide range of extracellular osmolarity and need potent volume regulatory mechanisms for the maintenance of cell volume and epithelial transport (for review, see Montrose-Rafizadeh and Guggino, 1990). In the present study we identified a swelling-activated Cl^- conductance in cultured M-1 mouse cortical collecting duct (CCD)[1] cells (Stoos et al., 1991) and attempted to classify functionally this conductance and the underlying single-channels within the emerging family of swelling-activated Cl^- channels.

Portions of this work were presented in abstract form (Meyer, K., E. Frömter, and C. Korbmacher. 1995. Hypotonicity activates a chloride conductance in M-1 mouse cortical collecting duct cells. *Pflügers Archiv.* 429[Suppl. 6]:R122).

Address correspondence to Dr. Christoph Korbmacher, Zentrum der Physiologie, Klinikum der Johann Wolfgang Geothe-Universität, Theodor Stern Kai 7, D-60590 Frankfurt am Main, Germany, Fax: 49-69-6301-7142; E-mail: korbmacher@em.uni-frankfurt.de

[1] *Abbreviations used in this paper.* CCD, cortical collecting duct; CFTR, cystic fibrosis transmembrane conductance regulator; NMDG, *N*-methyl-D-glucamine; VC, voltage clamp.

MATERIALS AND METHODS

Cell Culture

The M-1 cell line (Stoos et al. 1991) was used from passages 12 through 30 and cells were handled as described (Korbmacher et al. 1993; Letz et al., 1995). For patch clamp experiments cells were seeded onto small pieces of glass cover slips (Baxter Scientific Products, McGaw Park, IL) and were used one day after seeding. Whole-cell recordings were obtained from nonpolarized single cells which had no contact to neighboring cells.

Patch Clamp Technique

The ruptured-patch whole-cell configuration of the patch clamp technique was used (Hamill et al. 1981) and experimental procedures were essentially as described (Korbmacher et al. 1993; Letz et al. 1995). Cells were viewed through a 40× objective of a Nikon TMS inverted microscope (Nikon GmbH, Düsseldorf, Germany) equipped with Hoffman modulation optics (Modulation Optics Inc., Greenvale, NY), and cell diameter was estimated using a micrometer grid. Patch pipettes were pulled from Clark glass capillaries (Clark Electromedical Instruments, Pangbourne, UK). In NaCl-solution the resistance (R_{pip}) of pipettes filled with NMDG-Cl solution (see below) averaged 5.2 ± 0.1 MΩ (n = 232) with a range of 2–9 MΩ. Experiments were performed at room temperature. Currents were amplified with an EPC-9 patch clamp amplifier (HEKA Elektronik, Lambrecht, Germany). Whole-cell currents were recorded using the voltage clamp mode (VC) and membrane voltage (V_m) was observed by switching from VC to zero current clamp (CC) mode. Membrane capacitance (C_m) and series resistance (R_s) were estimated by nulling capacitive transients using the automated EPC-9 compensation circuit. R_s averaged 12.9 ± 0.4 MΩ (n = 232) and was compensated by 70%. In VC mode the cytoplasmic potential corresponds to the holding potential (V_{pip}) referenced to the bath. The reference electrode was an Ag/AgCl pellet bathed in the same solution as that used in the pipette and connected to the bath via an agar/pipette-solution bridge in the outflow path of the chamber. Liquid junction (LJ) potentials occurring at the bridge/bath junction were measured using a 3M KCl flowing boundary electrode and ranged from 5 to 23 mV. The V_{pip} settings and V_m values were corrected accordingly. Upward current deflections correspond to cell membrane outward currents, i.e., movement of positive charge from the cytoplasmic side to the extracellular side. Current data were recorded at 10 kHz bandwidth. For later analysis currents were filtered at 100–500 Hz using an 8-pole Bessel filter and sampled at a rate of 0.5–2 kHz. The overall cell conductance G_{cell} was estimated by calculating $G_{cell} = \Delta I/180$ mV where ΔI is the whole-cell (peak) current deflection observed upon stepping V_{pip} from −60 to +120 mV. Data are given as mean values ± SEM, significances were evaluated by the appropriate version of Student's *t test*.

Solutions and Chemicals

The initial bath solution in which giga-ohm seals were formed was NaCl-solution (in mM): 140 NaCl, 5 KCl, 1 $CaCl_2$, 1 $MgCl_2$ and 10 HEPES (adjusted to pH 7.5 with NaOH). To prevent cationic outward currents, the impermeable monovalent cation *N*-methyl-D-glucamine (NMDG) was used in all pipette solutions. To achieve "nonswelling" conditions (Worrell et al., 1989) the pipette solutions had slightly lower osmolarities than the corresponding bath solutions. In an initial set of experiments we used a 100-NMDG-Cl/EGTA pipette solution which contained (in mM): 100 NMDG-Cl, 50 sucrose, 1 $MgCl_2$, 1 ATP (magnesium salt), 1 EGTA, 10 HEPES (adjusted to pH 7.5 with Tris). The corresponding 100-NMDG-Cl bath solution contained: 100 NMDG-Cl, 100 sucrose, 1 Mg-gluconate, 1 Ca-gluconate, 10 HEPES (adjusted to pH 7.5 with Tris). In further experiments we used a 125-NMDG-Cl/EGTA pipette solution which contained (in mM): 125 NMDG-Cl, 25 sucrose, 1 $MgCl_2$, 1 ATP (magnesium salt), 1 EGTA, 10 HEPES (adjusted to pH 7.5 with Tris). The corresponding 125-NMDG-Cl bath solution contained: 125 NMDG-Cl 50 sucrose, 1 Mg-gluconate, 1 Ca-gluconate, 10 HEPES adjusted to pH 7.5 with Tris. Extracellular hypotonicity was achieved by completely removing the sucrose from the bath solutions without changing their ion composition. Extracellular Cl^- was removed by completely replacing bath Cl^- by gluconate. We also used a 125-NaCl bath solution which contained (in mM): 125 NaCl, 50 sucrose, 1 Mg-gluconate, 1 Ca-gluconate, 10 HEPES (adjusted to pH 7.5 with Tris). Anion selectivity was tested by replacing the 125 mM NaCl by an equal amount of NaI, NaBr, NaSCN, or Na-gluconate under hypotonic conditions. All bath solutions contained 5 mM glucose. Ca^{2+} free bath solutions were obtained by omitting Ca-gluconate and by adding 1 mM EGTA. Furthermore, in some experiments the pipette solution contained 10 mM instead of 1 mM EGTA and sometimes, in addition, 2 μM thapsigargin or 0.1 mM TMB-8 (8-(*N,N*-diethylamino)octyl 3,4,5-trimethoxybenzoate). In one set of experiments, cells were ATP-depleted by a 20–45 min preincubation in NaCl-bath solution containing 100 nM rotenone and 5 mM 2-deoxyglucose instead of glucose. A similar preincubation protocol has previously been shown to deplete effectively lung cancer cells from intracellular ATP. In these cells a 10-min preincubation in 100 nM rotenone and 10 mM 2-deoxyglucose depleted intracellular ATP levels to <5% of control levels (Jirsch et al., 1994). During the patch-clamp experiments the ATP-depleted M-1 cells were kept in the continuous presence of rotenone and 2-deoxyglucose in the bath and pipette solution. Ionomycin, TMB-8, and thapsigargin were from Calbiochem (Bad Soden, Germany). NPPB (5-nitro-2(3-phenylproplylamino)-benzoate) was a generous gift from Hoechst Pharmaceutical Co. (Hoechst, Germany). All other drugs and chemicals were obtained from Sigma (Deisenhofen, Germany). Water-insoluble substances were dissolved in DMSO, except for tamoxifen, which was dissolved in ethanol. The final DMSO concentration did not exceed 0.1%. The final ethanol concentration was maximally 1% at which ethanol had no significant effect on the whole-cell Cl^- currents activated by hypotonicity.

RESULT

Whole-cell Recordings in M-1 Cells

In single nonpolarized M-1 cells 24 h after seeding, giga-ohm seals were obtained in about two out of three attempts. Following giga-ohm seal formation the ruptured-patch whole-cell configuration was achieved in ~70% of the attempts. The cell membrane capacitance (C_m) averaged 9.0 ± 0.3 pF (n = 232) within the first min after achieving the whole-cell configuration. Giga-ohm seals could be maintained for up to 2 h. This made it possible to perform solution exchanges and to apply drugs while monitoring V_m or whole-cell currents in (VC) or in zero current clamp (CC) mode, respectively.

Extracellular Hypotonicity Stimulates a Cl^- Conductance

The continuous whole-cell current recording shown in Fig. 1 was obtained in the presence of symmetrical 100 mM NMDG-Cl in the bath (100-NMDG-Cl solution)

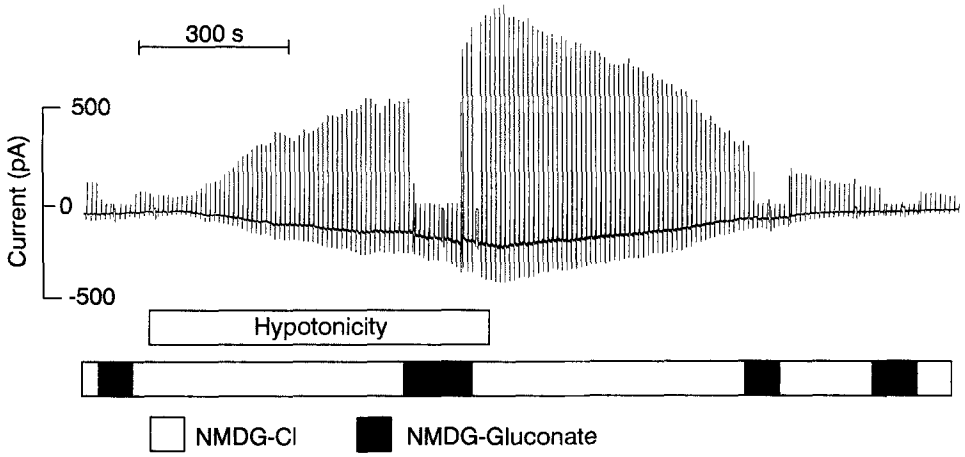

FIGURE 1. Hypotonicity stimulates whole-cell Cl^- currents. A continuous whole-cell current recording in the presence of symmetrical 100 mM NMDG-Cl in the bath (100-NMDG-Cl solution) and in the pipette (100-NMDG-Cl/EGTA solution) is shown; 2-s voltage ramps from −120 mV to +120 mV were repetitively applied. Extracellular hypotonicity was achieved by removing 100 mM sucrose from the bath solution without changing its ionic composition. Extracellular NMDG-Cl was replaced by NMDG-gluconate as indicated.

and in the pipette (100-NMDG-Cl/EGTA solution). Most ion channels are impermeable to the large organic cation NMDG (*N*-methyl-D-glucamine). Thus, under the chosen experimental conditions the major charge carrying ion was Cl^-. Under voltage clamp conditions 2-s voltage ramps from −120 to +120 mV were repetitively applied. Extracellular hypotonicity was achieved by removing 100 mM sucrose from the bath solution. As shown in Fig. 1 both inward and outward whole-cell currents began to increase 64 ± 4 s (n = 18) after changing to hypotonic bath solution and continued to increase in its presence. The effect was reversible after changing back to the original bath solution containing 100 mM sucrose. The stimulated outward currents were considerably larger than the stimulated inward currents indicating that the underlying conductance is outwardly rectifying. Replacement of extracellular Cl^- by gluconate almost completely abolished the outward current, indicating that the stimulated current is carried by Cl^- influx. Fig. 2 shows current traces and *I-V* curves obtained from voltage-step protocols performed during a similar experiment as the one shown in Fig. 1. In hypotonic solutions, the stimulated whole-cell currents showed a characteristic time-dependent decay during large depolarizing voltage steps and a small but significant continuous increase during hyperpolarizing voltage steps (Fig. 2 *A*). During 400-ms voltage steps to −90 and −120 mV inward currents increased on average by 2.7 ± 0.4% (n = 41; $P \leq 0.001$) and 10.0 ± 1.1% (n = 41; $P \leq 0.001$), respectively. Under non-swelling conditions no such hyperpolarization-induced current increase occurred. Fig. 2 *B* shows *I-V* curves under hypotonic conditions in the presence and absence of extracellular Cl^- that are derived from the current traces shown in Fig. 2 *A*. Current data were taken from the early portion of each current trace at 15 ms of the pulse onset. Replacement of extracellular Cl^- by gluconate shifted the reversal potential from −1 to +92 mV, indicating that the currents were selectively carried by Cl^-.

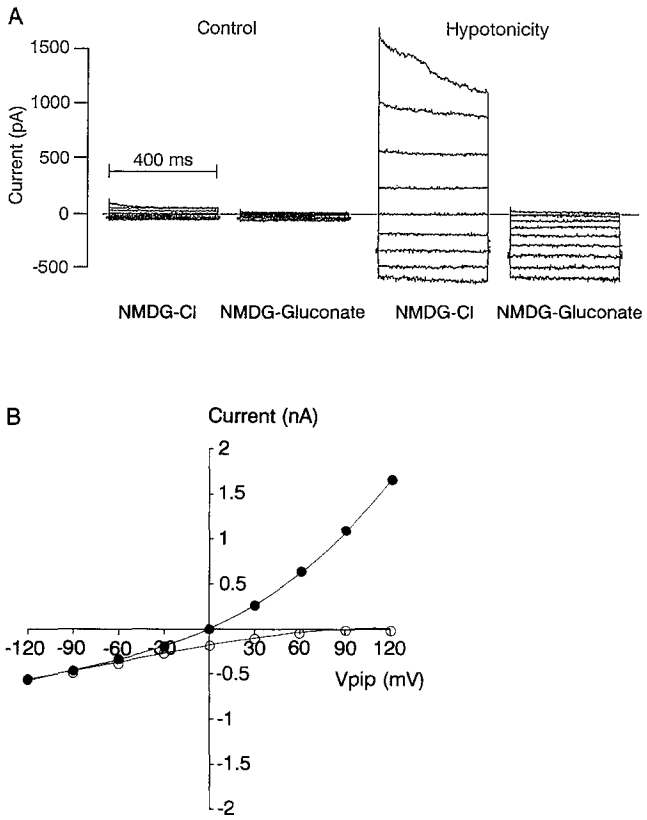

FIGURE 2. The swelling-activated whole-cell currents are outwardly rectifying. The current traces (*A*) and *I-V* curves (*B*) were obtained from voltage step protocols performed during a similar experiment as the one shown in Fig. 1. In (*A*) an overlay of 9 individual whole-cell current traces is displayed for each condition, resulting from consecutive 400-ms voltage steps in 30 mV increments starting with a hyperpolarizing pulse to −120 mV from a holding potential of −60 mV. After each pulse the holding potential was returned to −60 mV for about 1 s. (*B*) Current data were taken from the early portion of the current traces (15 ms into the pulse) to construct *I-V* curves from the whole-cell current data during hypotonic activation in the presence (*closed circles*) and absence (*open circles*) of extracellular Cl^- which was replaced by gluconate. Current traces under stimulated conditions were recorded 10 min after changing to hypotonic bath solution.

TABLE I

Effects of Hypotonicity on Cell Conductance (G_{cell}) and Cell Diameter

	G_{cell}	Diameter
	nS	*μm*
Control	0.39 ± 0.04	15.4 ± 0.5
	(n = 52)	(n = 19)
Hypotonic	12.10 ± 1.17*	19.9 ± 0.5*
	(n = 52)	(n = 19)
Wash	0.50 ± 0.08	14.3 ± 0.7
	(n = 21)	(n = 11)

*Significantly different from control values in paired t test with $P < 0.001$.

Under the experimental conditions used in Fig. 1 and Fig. 2, the stimulated whole-cell currents did not reach a stable maximum, and giga-ohm seals were often lost during prolonged exposure to hypotonic bath solution, probably as a result of excessive hypotonic cell swelling induced by the removal of 100 mM sucrose. Therefore, we decided to use a smaller osmotic gradient to stimulate the conductance. In the following experiments the pipette contained 125 mM NMDG-Cl (125-NMDG-Cl/EGTA solution) and the bath solution contained 125 mM NaCl (125-NaCl solution). Extracellular hypotonicity was achieved by removing 50 mM sucrose from the bath solution. This also resulted in substantial cell swelling and whole-cell current activation which began 71 ± 6 s (n = 42) after changing to the hypotonic bath. Under these conditions whole-cell currents reached a stable maximum after 16 ± 1 min (n = 41), which could be maintained for a prolonged period of time under continuous hypotonic conditions. To speed up the recovery from hypotonic swelling, the hypotonic bath solution was usually washed out with a hypertonic 125-NaCl solution containing 100 mM sucrose until the cells had reached their original size as judged from the cell diameter. Subsequently the bath solution was changed back to the original 125-NaCl solution containing 50 mM sucrose. Whole-cell currents started to decline 33 ± 3 s (n = 17) after washout of the hypotonic solution and fully recovered 12 ± 1 min after washout (n = 14). Results from these experiments are summarized in Table I. On average the overall cell conductance (G_{cell}) increased in hypotonic solutions by >30-fold from 0.39 nS to a maximum of 12.1 nS. Cell diameter also increased significantly, on average by 4.6 ± 0.4 μm (n = 19, $P \leq 0.001$) which corresponds to a 30% increase (Table I). The apparent change in cell size always preceded the corresponding change of the whole-cell conductance. During maximal hypotonic activation with 125-NMDG-Cl/EGTA solution in the pipette and 125-NaCl solution without sucrose in the bath V_m averaged 0.3 ± 0.2 mV (not significantly different from zero) and shifted to 86.3 ± 1.2 mV upon extracellular Cl^- removal (n = 52). This indicates that the cells did not develop any significant nonselective leak conductance or Na^+ conductance under hypotonic conditions and confirmed that the stimulated whole-cell currents were almost exclusively carried by Cl^- with a permeability ratio $P_{Cl}/P_{gluconate}$ of 0.03.

Voltage Dependence of the Stimulated Conductance

The voltage dependence of $I_{Cl\text{-}swell}$ was investigated in experiments as shown in Figs. 3 and 4. Fig. 3 *A* represents a whole-cell current trace induced by a 2-s voltage pulse from a holding potential of −60 mV to a pulse potential of +120 mV under hypotonic conditions with symmetrical 100 mM NMDG-Cl in bath and pipette solution. The peak outward current was reached instantaneously upon stepping to +120 mV and subsequently

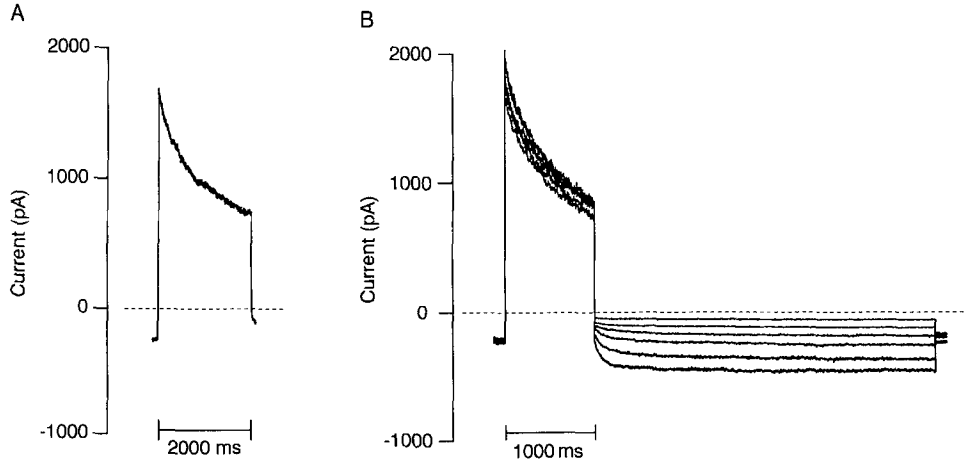

FIGURE 3. Whole-cell currents inactivate during depolarizing voltage steps and reactivate at hyperpolarizing potentials. (*A*) Current trace induced by a prolonged depolarizing voltage pulse of 2-s duration from a holding potential of −60 mV to a pulse potential of +120 mV under hypotonic conditions with symmetrical 100 mM NMDG-Cl in bath and pipette solution as in Figs. 1 and 2. After 2 s the potential was stepped back from +120 mV to the holding potential of −60 mV. (*B*) Whole-cell currents were recorded during steady state hypotonic activation after removing 50 mM extracellular sucrose with symmetrical 125 mM NMGD-Cl in the pipette (125-NMDG-Cl/EGTA solution) and in the bath (125-NMDG-Cl solution). An overlay of six consecutive current traces is shown. At the end of a fixed 1,000-ms prepulse from a holding potential of −60 to +120 mV the potential was then stepped for 4 s to various test potentials ranging from −20 to −120 mV in 20 mV increments.

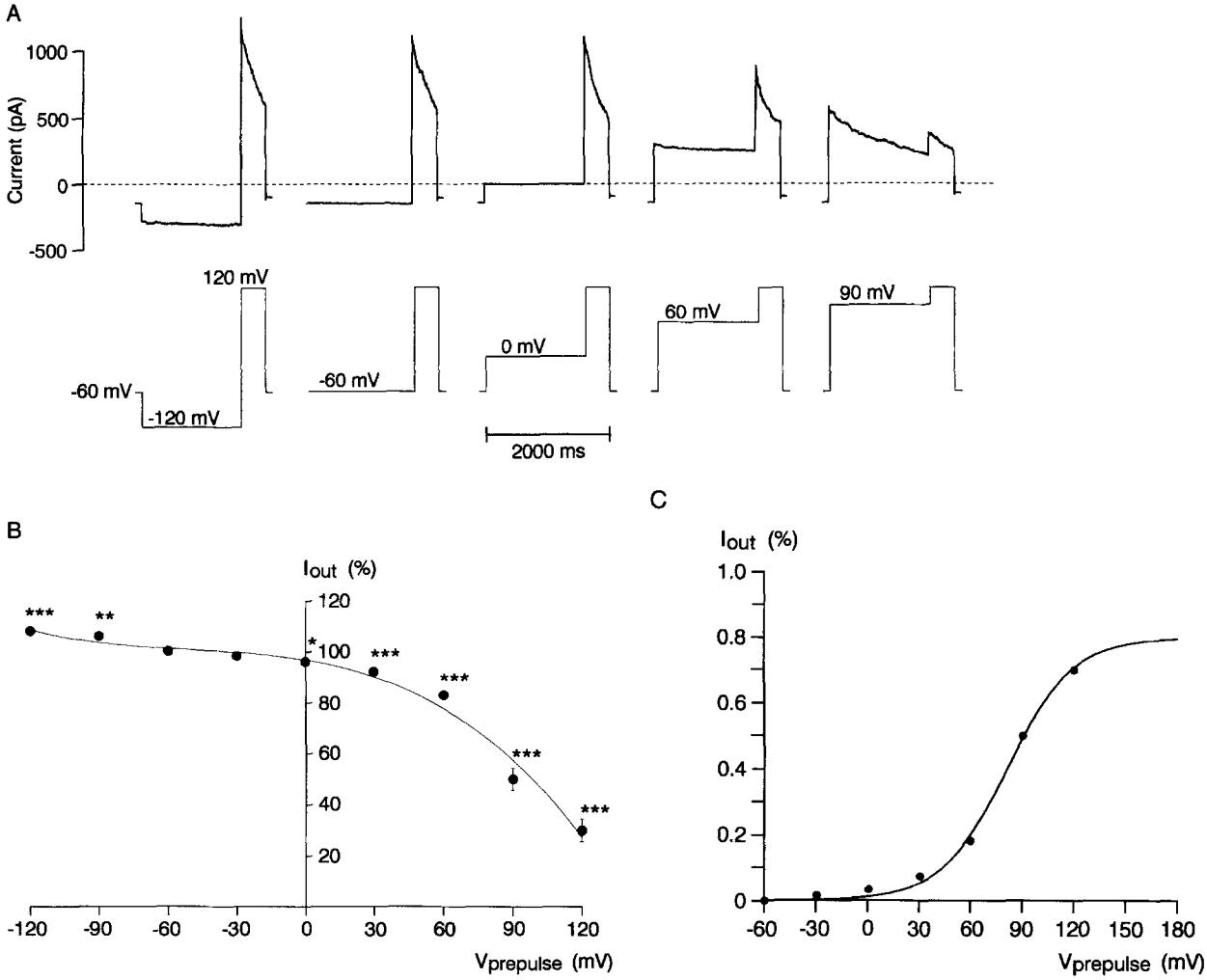

FIGURE 4. Voltage dependence of instantaneous outward currents. During maximal hypotonic activation a two-pulse voltage-clamp protocol was applied with a 1,600-ms prepulse from a holding potential of −60 mV to potentials ranging from −120 to +120 mV in 30 mV increments followed by a 400-ms test pulse to +120 mV. (*A*) Five individual whole-cell current traces are shown from a representative experiment. The pulse protocols are indicated below each current trace. Pipette solution was 125-NMGD-Cl/EGTA solution, and bath solution was 125-NaCl solution. Extracellular hypotonicity was achieved by removing 50 mM sucrose form the bath solution. (*B*) From seven similar experiments as shown in *A*, the average normalized instantaneous outward current I_{out} (%) is plotted versus the prepulse potential ($V_{prepulse}$). The instantaneous outward currents were measured 15 ms into the test pulse, and current values were normalized to the outward current measured after the prepulse to −60 mV. Values significantly different from this reference outward current are indicated by asterisks (*, **, *** for $P < 0.05$, $P < 0.01$, and $P < 0.001$, respectively; bars indicate SEM values ($n = 7$). (*C*) Using the same data as shown in *B* the inactivated fraction of the instantaneous outward current is plotted versus $V_{prepulse}$. A Boltzmann-fit of the data is shown and reveals a maximal inactivation of 80% with an inactivation midpoint at 73 mV and an effective gating charge of 1.3.

decayed during the 2-s sustained depolarization on average by 59.7 ± 2.2% ($n = 42$). The observed current decay could not be fitted with a single exponential function and remained incomplete even after 2 s of sustained depolarization. Upon return to the holding potential of −60 mV the inward tail current (10 ms after stepping back to −60 mV) was reduced (Fig. 3 *A*) on average by 53 ± 2.1% ($n = 42$) as compared to the inward current at −60 mV immediately prior to the depolarizing pulse. The decreased inward tail current confirms that channel inactivation had occurred during the depolarizing command pulse. Fig. 3 *B* demonstrates that channels reactivated after stepping back to hyperpolarizing holding potentials in a voltage-dependent manner. Reactivation occurred already at a holding potential of −20 mV but was faster at more negative potentials. The voltage dependence of channel activation and inactivation was further investigated in experiments illustrated in Fig. 4 using a two-pulse voltage-clamp protocol. The first 1,600-ms voltage step, the variable "prepulse" or "conditioning pulse," was intended to permit the voltage-dependent process to approximately reach a "steady-state" level at the prepulse potential. The second voltage step, the "test pulse," to a fixed level of +120 mV elicited the usual instantaneous Cl^- outward current whose relative amplitude was used

TABLE II

Effect of Extracellular Chloride Replacement by Various Anions on Reversal Potential (E_{rev}) and Outward Conductance (G_{out}) during Hypotonic Stimulation

	ΔE_{rev}	P_X^-/P_{Cl}^-	$G_{out\text{-}15\text{-}ms}$	$G_{out\text{-}400\text{-}ms}$	n
	mV		%	%	
Cl^-	0	1	100	100	8
gluconate	81.5 ± 1.1*	0.04	4.9 ± 0.6*	4.5 ± 0.5*	8
SCN^-	−13.1 ± 0.6*	1.68	87.1 ± 2.7‡	162.9 ± 23.4§	8
I^-	−9.6 ± 0.5*	1.46	98.4 ± 7.9n.s.	145.6 ± 20.0n.s.	8
Br^-	−4.6 ± 0.2*	1.20	101.9 ± 1.8n.s.	102.9 ± 8.7n.s.	7

n.s. Not significantly different from control in Cl^-. *, ‡, §Significantly different from control in Cl^- with $P < 0.001$, $P < 0.01$, and $P < 0.05$, respectively. ΔE_{rev}, shift of reversal potential induced by a test-anion which was calculated by subtracting the membrane voltage (V_m) measured in the presence of Cl^- from that measured in the presence of a test-anion. The reported values have been corrected for liquid junction potentials (see MATERIALS AND METHODS). P_X^-/P_{Cl}^-, ratio of permeability of test-anion (P_X^-) to permeability of Cl^- (P_{Cl}^-) which was calculated according to the following equation:

$$\Delta E_{rev} = \frac{RT}{zF} \cdot \ln \frac{P_{X^-} \cdot [X^-]_o}{P_{Cl^-} \cdot [Cl^-]_o}.$$

TABLE III

Effects of Anion Substitution and Inhibitors on Outward Current Inactivation (ΔI_{out}) during Depolarizing Voltage Steps from −60 to 120 mV

	Control in Cl^-	Test	n
	ΔI_{out} %/100 ms	ΔI_{out} %/100 ms	
Anions			
SCN^-	13.1 ± 0.9	0.6 ± 1.7*	8
I^-	14.5 ± 1.9	5.4 ± 1.5‡	8
Br^-	14.0 ± 1.6	10.6 ± 1.1‡	7
Inhibitors			
NPPB (100 μM)	13.9 ± 1.2	35.2 ± 2.4*	9
DIDS (100 μM)	9.8 ± 1.9	35.2 ± 3.6*	5
Tamoxifen (10 μM)	11.4 ± 2.0	30.7 ± 4.8‡	7
Verapamil (100 μM)	13.0 ± 2.1	17.0 ± 3.0‡	6
Glibenclamide (100 μM)	13.3 ± 1.4	34.0 ± 1.9‡	15
Flufenamic acid (100 μM)	12.2 ± 1.5	45.2 ± 1.9*	10

*,‡Significantly different from control values with $P < 0.001$ and $P < 0.01$, respectively.

to determine what fraction of the current was activated or inactivated by the preceding prepulse. After depolarizing prepulses to 0 mV or more positive potentials the instantaneous outward currents were significantly decreased with a rather steep voltage dependence of channel inactivation between +30 and +120 mV as illustrated in Fig. 4 *B*, which summarizes results from seven experiments similar to that shown in Fig. 4 *A*. In contrast, after hyperpolarizing prepulses to −90 or −120 mV, the instantaneous Cl^- outward currents were slightly, but significantly, increased, indicating that even at −60 mV the underlying Cl^- channels are partially inactivated and can be further activated by hyperpolarization ($n = 7$, Fig. 4 *B*). It is commonly believed that voltage sensitivity is conferred by charged residues that move through the membrane potential field in response to changes in membrane potential. The steepness of the voltage dependence of inactivation can be used to estimate the effective gating charge by fitting the Boltzmann equation to the data as shown in Fig. 4 *C*. The parameters derived from this fit are a maximal inactivation of 80% with an inactivation midpoint at 73 mV and an effective gating charge of 1.3. However, since steady state current levels were not fully reached during the prepulses, we probably underestimate the steepness of inactivation. Thus, it is likely that the effective gating charge is at least 2.

Anion Selectivity of the Stimulated Conductance

During steady state hypotonic activation the anion selectivity of the stimulated whole-cell conductance was tested by replacing 125 mM NaCl in the bath solution by an equimolar amount of Na^+ salts of gluconate, SCN^-, I^-, or Br^- (Fig. 5). Outward conductances and reversal potentials were determined in the presence of each anion and compared to the corresponding values in the presence of Cl^- before and after the application of the test-anion. Results are summarized in Table II. The permeability sequence derived from these reversal potential data (Table II) is the following: $SCN^- > I^- > Br^- > Cl^- > >$ gluconate. The conductance sequence was determined by evaluating outward conductances from whole-cell current data as shown in Fig. 5. The whole-cell outward currents measured during voltage pulses to +90 and +120 mV were used to estimate G_{out} according to $G_{out} = \Delta I/30$ mV, where ΔI is the difference of the whole-cell currents measured at +120 and +90 mV. As can be seen in Fig. 5, the test-anions not only affected the overall magnitude of the outward currents but also the time course of current inactivation during depolarizing voltage steps. Therefore, we calculated an initial outward conductance ($G_{out\text{-}15\text{-}ms}$), using the current data recorded at the beginning of each voltage pulse (15 ms into the pulse), and a late outward conductance at the end of each 400-ms pulse ($G_{out\text{-}400\text{-}ms}$). The conductance sequence derived from the initial conductances is $I^- \approx Br^- \approx Cl^- > SCN^- > >$ gluconate. In contrast, the conductance sequence according to the conductances measured at the end of the 400-ms pulses is $SCN^- > I^- > Br^- \geq Cl^- > >$ gluconate, which corresponds well with the permeability sequence obtained from the reversal potential data. The effect of the various anions on channel inactivation was quantified by estimating the relative initial outward current decay during a depolarizing voltage step to +120 mV (from 15 to 115 ms into the pulse). These values were

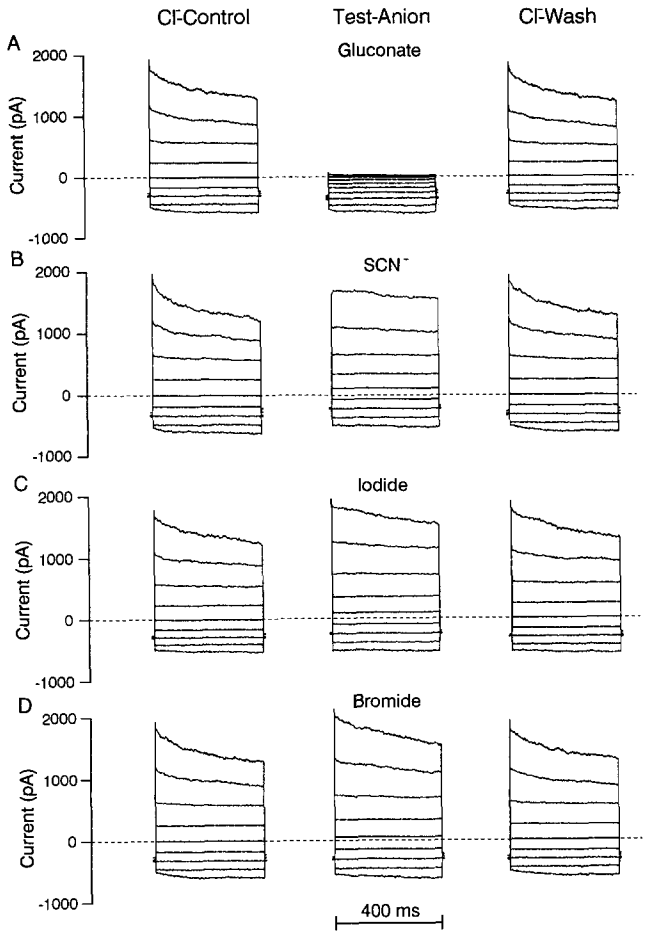

FIGURE 5. Anion selectivity of the swelling-activated conductance. During maximal hypotonic activation of whole-cell currents extracellular Cl^- was removed and was replaced by different test-anions. Representative whole-cell current traces from four different experiments are shown using as test-anions gluconate (*A*), SCN^- (*B*), iodide (*C*), or bromide (*D*). An overlay of nine individual whole-cell current traces is displayed for each condition (*Cl^- control, test-anion, Cl^- wash*), resulting from consecutive 400-ms voltage steps in 30 mV increments starting with a hyperpolarizing pulse to −120 mV from a holding potential of −60 mV. After each pulse the holding potential was returned to −60 mV for about 1 s.

compared with the corresponding decay in the presence of Cl^- measured in the same experiments. Table III (top) summarizes these results. Relative outward current inactivation was slowest in the presence of SCN^- followed by I^-, Br^-, and Cl^-. This indicates that the gating mechanism responsible for channel inactivation is affected by the anions permeating the channel.

Effect of Inhibitors on $I_{Cl\text{-}swell}$

Various drugs and inhibitors known to affect Cl^- conductances in other systems were tested. Their effects on $I_{Cl\text{-}swell}$ are summarized in Table IV and whole-cell current traces from representative experiments, illustrating the inhibitory action of tamoxifen, NPPB, DIDS, and glibenclamide, are shown in Fig. 6. Tamoxifen was the most potent inhibitory substance, but the time course of tamoxifen action was much slower than that of the other drugs used. This may indicate that tamoxifen has to accumulate in the cell membrane in order to inhibit the channel. Maximal current inhibition by tamoxifen was observed 164 ± 13 s (n = 10) after its application and currents recovered within 318 ± 33 s (n = 7) after washout. In some experiments recovery remained incomplete. In contrast, with NPPB maximal inhibition was reached within 29 ± 1 s after application and washout of the effect was complete within 63 ± 6 s (n = 9). The time course of the inhibitory effect of the other inhibitors was similar to that of NPPB. Tamoxifen inhibited inward and outward currents equally. NPPB and most of the other inhibitory substances reduced both inward and outward currents but with a preferential inhibition of outward currents. As can be seen in Fig. 6, DIDS and glibenclamide reduced almost exclusively outward currents with only minor effects on inward currents. A similar voltage-dependent inhibitory pattern of DIDS has previously been reported for the osmotically activated Cl^- currents in T-lymphocytes and has been interpreted as an interaction of the doubly charged anion DIDS with multiple binding sites within the membrane electric field (Lewis et al., 1993). This interpretation could also be used for glibenclamide, which is a weak acid and is likely to be negatively charged at pH 7.5. Glibenclamide, a known blocker of ATP-sensitive K^+ channels, has been shown to effectively inhibit various Cl^- channels (Wangemann et al., 1986; Rabe et al., 1995; Volk et al., 1995*b*) including CFTR (cystic fibrosis transmembrane conductance regulator) (Sheppard and Welsh, 1992). Flufenamic acid and niflumic acid, derivatives of the Cl^- channel blocker DPC (diphenylcarboxylate), also inhibited $I_{Cl\text{-}swell}$. Again, the effect of flufenamic acid, which at pH 7.5 is negatively charged, appeared to be more pronounced on outward currents than on inward currents. Verapamil (10^{-4} M) reduced the stimulated Cl^- conductance only by ~ 19%. The cyclic nucleotide cAMP, and acycloguanosine (Acyclovir; 9-[(2-hydroxyethoxy)methyl]guanine) had only minor effects on $I_{Cl\text{-}swell}$. Interestingly, as can be seen in Fig. 6 and as summarized in Table III (bottom), the current decay during depolarizing voltage steps was significantly faster in the presence of all effective inhibitory substances used. This suggests that the inhibitors modulate the voltage-dependent channel gating in an opposite way as the anions listed in the top of Table III. One certainly expects that negatively charged blockers like DIDS may increase the apparent rate of inactivation since at depolarizing voltages, the rate of current reduction will be a function of both the "on" rate of the drug and the rate of voltage-sensitive inactivation. However, it was surprising that voltage-independent block-

TABLE IV

Effect of Inhibitors on the Swelling-induced Whole-cell Conductance (G_{cell})

Inhibitor	Concentration	Inhibition of G_{cell}	n
		%	
NPPB	100 μM	72 ± 3*	8
	10 μM	14 ± 7	5
	1 μM	2 ± 5	5
	0.1 μM	1 ± 3	5
DIDS	100 μM	55 ± 1*	5
	50 μM	40 ± 5‡	6
	5 μM	8 ± 2§	4
Tamoxifen	10 μM	73 ± 4*	7
	1 μM	10 ± 9	5
	0.1 μM	10 ± 5	5
Verapamil	100 μM	19 ± 4*	6
Glibenclamide	100 μM	23 ± 2*	10
	10 μM	2 ± 2	10
	1 μM	2 ± 2	10
Flufenamic acid	100 μM	58 ± 2*	9
	10 μM	7 ± 2§	12
	1 μM	0 ± 2	12
Niflumic acid	50 μM	24 ± 6‡	6
Acycloguanosine	100 μM	11 ± 2‡	4
cAMP	1 mM	12 ± 4	3

*,‡,§Significantly different from control with $P < 0.001$, $P < 0.01$, and $P < 0.05$, respectively.

ers like tamoxifen also increased the rate of inactivation during depolarization. This suggests that inhibitor binding may allosterically alter channel gating.

Effect of Extracellular pH on the Stimulated Cl^- Conductance

It has been previously reported that extracellular pH modulates the inactivation kinetics of $I_{Cl\text{-}swell}$ in *Xenopus laevis* oocytes (Ackerman et al., 1994) and in rat glioma cells (Jackson and Strange, 1995*a*). However, in M-1 cells changing extracellular pH during steady state hypotonic activation from 7.5 to 6.5 or 8.5 did not significantly affect the magnitude of $I_{Cl\text{-}swell}$ nor its inactivation kinetics. When extracellular pH was reduced from 7.5 to 6.5 the outward currents at 120 mV averaged 1,630 ± 456 pA and 1,675 ± 487 pA, respectively, and the corresponding inactivation rates were 15.3 ± 2.1%/100 ms and 14.7 ± 1.6%/100 ms (n = 8). When extracellular pH was increased from 7.5 to 8.5, the outward currents at 120 mV averaged 1,930 ± 501 pA and 1,937 ± 505 pA, respectively, and the corresponding inactivation rates were 13.4 ± 1.5%/100 ms and 13.0 ± 1.6%/100 ms (n = 8).

Role of Calcium

A transient rise of intracellular Ca^{2+} concentration in response to hypotonic cell swelling has been observed in a number of systems including the collecting duct (Tinel et al., 1994; Fu et al., 1995), and may play a role

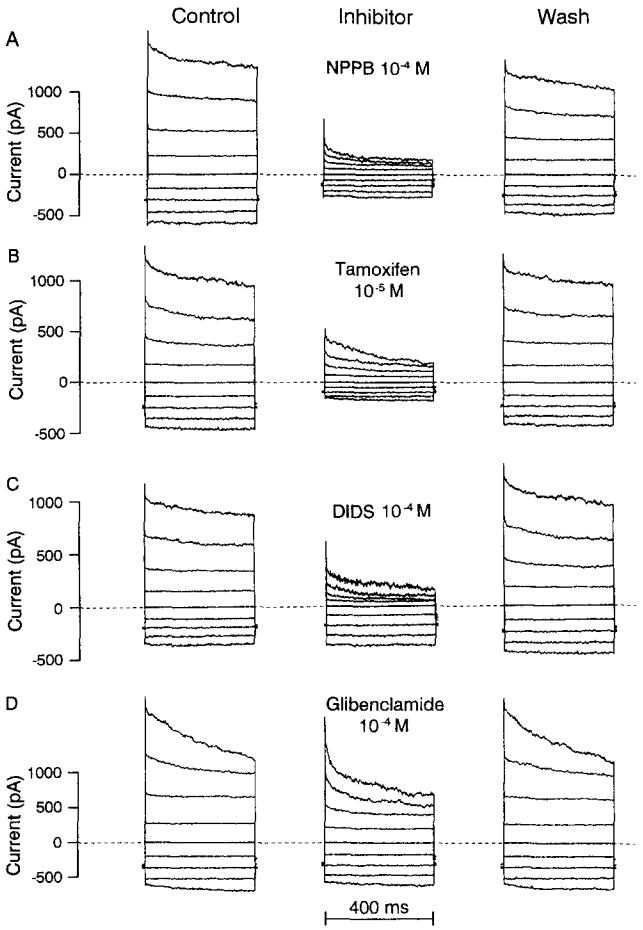

FIGURE 6. Effect of inhibitors on the swelling-activated conductance. During maximal hypotonic activation of whole-cell currents the effect of various inhibitors was tested. Representative whole-cell current traces from four different experiments are shown using as inhibitors NPPB 10^{-4} M (*A*), tamoxifen 10^{-5} M (*B*), DIDS 10^{-4} M (*C*), or glibenclamide 10^{-4} M (*D*). An overlay of nine individual whole-cell current traces is displayed for each condition (*control, inhibitor, wash*). The same voltage-step protocol was used as described in legend of Fig. 5.

for the activation of $I_{Cl\text{-}swell}$. In most systems this rise in intracellular Ca^{2+} is at least partially dependent on the presence of extracellular Ca^{2+} (for review, see McCarty and O'Neil, 1992). Therefore, we tested the effect of Ca^{2+} removal during steady-state hypotonic activation of the Cl^- conductance. Extracellular Ca^{2+} removal neither affected the magnitude of the stimulated current nor the time course of the outward current inactivation during depolarization. In the presence and absence of extracellular Ca^{2+} the outward currents at 120 mV averaged 855 ± 224 pA and 825 ± 234 pA, respectively, and the corresponding inactivation rates were 14.4 ± 2.3%/100 ms and 14.3 ± 2.0%/100 ms (n = 5).

We also investigated whether Ca^{2+} release from intracellular stores may be involved in the activation of $I_{Cl\text{-}swell}$. In an attempt to buffer effectively intracellular Ca^{2+} signals we used a Ca^{2+}-free pipette solution containing 10

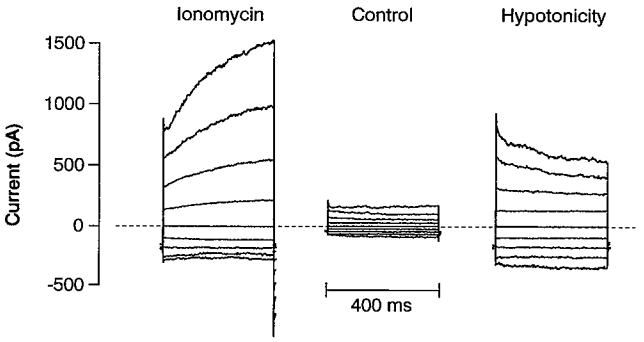

FIGURE 7. Calcium-activated Cl^- conductance and calcium-independent swelling-activated Cl^- conductance. In this experiment the pipette solution was 125-NMDG-Cl/EGTA solution with a free Ca^{2+} concentration of 10^{-7} M. The initial bath solution was 125-NaCl solution. Application of 1 μM ionomycin in the presence of 1 mM Ca^{2+} in the bath activated large Cl^- currents (*left traces, Ionomycin*). Whole-cell currents recovered back to baseline after washout of ionomycin with a Ca^{2+} free 125-NaCl/EGTA solution (*middle traces, Control*). In the continuous absence of extracellular Ca^{2+} removal of 50 mM sucrose activated $I_{Cl\text{-}swell}$ (*right panel, Hypotonicity*). An overlay of nine individual whole-cell current traces is shown for each experimental period. The same voltage-step protocol was used as described in legend of Fig. 5.

mM EGTA instead of the usual 1 mM EGTA, and the experiments were carried out in Ca^{2+}-free bath solutions containing 1 mM EGTA throughout the experiment. Under these conditions G_{cell} increased from 0.47 ± 0.21 to 7.04 ± 0.76 nS upon exposure to hypotonic bath solution (n = 7; $P \leq 0.001$). Moreover, experiments were performed in which the Ca^{2+}-free pipette solution contained 10 mM EGTA and in addition 2 μM thapsigargin or 100 μM TMB-8 in order to block or deplete intracellular Ca^{2+} stores, respectively. With TMB-8 or thapsigargin in the pipette, exposure to hypotonic bath solution increased G_{cell} from 0.46 ± 0.18 nS to 13.06 ± 1.82 nS (n = 4, $P \leq 0.01$) or from 0.40 ± 0.17 nS to 13.39 ± 3.02 nS (n = 5, $P \leq 0.001$), respectively. Thus, under all these conditions exposure to hypotonic solutions resulted in a normal activation of $I_{Cl\text{-}swell}$.

Interestingly, channel inactivation during depolarizing voltage steps was significantly faster in the experiments in which the pipette solution contained 10 mM EGTA, compared to the inactivation observed with the usual 1 mM EGTA in the pipette solution. The initial outward current decay (from 15 to 115 ms into the pulse) during a depolarizing voltage step to +120 mV averaged 16.3 ± 1.7%/100 ms (n = 16) with 10 mM EGTA compared to 12.3 ± 0.5%/100 ms (n = 92) with 1 mM EGTA in the pipette solution. Thus, the kinetics of channel inactivation seem to be modulated by increasing the intracellular buffering capacity for Ca^{2+}. Nevertheless, our data indicate that the activation mechanism of $I_{Cl\text{-}swell}$ in M-1 cells is independent of intra- or extracellular Ca^{2+}.

When intracellular Ca^{2+} was increased using the Ca^{2+} ionophore ionomycin (1 μM), a typical calcium-activated Cl^- conductance could be activated in M-1 cells (Fig. 7) which had an appearance similar to calcium-activated Cl^- conductances described in other systems (Kubo and Okada, 1992; Ackerman et al. 1994). These calcium-activated Cl^- currents showed a rather slow activation during depolarizing voltage pulses and subsequently a fast inactivation upon stepping back to −60 mV. The experiment shown in Fig. 7 demonstrates that after washout of ionomycin using a Ca^{2+}-free bath solution exposure to hypotonic solution elicits normal $I_{Cl\text{-}swell}$. The calcium-activated Cl^- currents can be distinguished from $I_{Cl\text{-}swell}$ by the different voltage dependence of channel activation and inactivation.

ATP Dependence of the Stimulated Cl^- Conductance

An ATP dependence of $I_{Cl\text{-}swell}$ has previously been demonstrated in a variety of cell types (Doroshenko and Neher, 1992; Lewis et al., 1993; Jackson et al., 1994; Jirsch et al., 1994; Oike et al., 1994; Jackson et al., 1996). We therefore investigated the role of intracellular ATP for the whole-cell current response to hypotonicity in M-1 cells. To this end we used ATP-depleted cells (see MATERIAL AND METHODS) which were kept in the continuous presence of 100 nM rotenone and 5 mM 2-deoxyglucose throughout the experiment. Rotenone and 2-deoxyglucose were added to the pipette solution and also to the bath solutions which contained no glucose. The results from these experiments are summarized in Table V. In ATP-depleted cells dialyzed with an ATP-free pipette solution, the usual whole-cell conductance increase in response to hypotonic cell swelling was almost completely absent. However, if the pipette solution was supplemented with 1 mM ATP, the whole-cell

TABLE V

Effect of Different Pipette Solutions on the Response of ATP-depleted Cells to Hypotonic Cell Swelling

Pipette solution*	Control G_{cell}	Hypotonic G_{cell}	n
	nS	*nS*	
ATP-free	0.20 ± 0.03	0.37 ± 0.06	12
ATP	0.46 ± 0.10	9.38 ± 0.96	12
Mg^{2+}-free‡, ATP	0.99 ± 0.19	2.51 ± 0.46	5
ATPγS	0.70 ± 0.07	7.54 ± 1.60	5
AMP-PNP	0.24 ± 0.03	0.95 ± 0.16	7
GTP	0.55 ± 0.28	1.78 ± 0.45	6
Staurosporine§, ATP	0.35 ± 0.08	2.64 ± 0.45	7

*Cells were ATP-depleted as described in MATERIALS AND METHODS and pipettes were filled with 125-NMDG-Cl/EGTA pipette solution containing 100 nM rotenone and 5 mM 2-deoxyglucose. Pipette solution was modified as indicated, the nucleotides were included in a concentration of 1 mM. ‡Mg^{2+}-free pipette solution contained 1 mM EDTA instead of 1 mM EGTA and ATP was added as sodium salt. §Cells were pretreated for 30–45 min with 5 nM staurosporine which was subsequently also included in the pipette and bath solution.

current response to hypotonicity was restored in ATP-depleted cells, and $I_{Cl\text{-}swell}$ reached similar values as in control cells. This rescuing effect of ATP was dependent on the presence of magnesium, indicating that an enzymatic reaction requiring magnesium as a cofactor may be involved. Using 1 mM ATPγS (adenosine 5′-*O*-[3-thiotriphosphate]) in the pipette solution was almost as effective as using 1 mM ATP. ATPγS is known to substitute for ATP in many kinase reactions. In contrast, 1 mM of the nonhydrolyzable ATP analogue AMP-PNP (5′-adenylimidodiphosphate) failed to restore the response to hypotonicity, indicating that a high energy gamma-phosphate group is necessary in the chain of events leading to channel activation. The effect of ATP and ATPγS could not be mimicked by GTP. We also tested the effect of staurosporine, a rather unspecific protein kinase C inhibitor which also affects other kinases. Cells were pretreated for 30–45 min with 5 nM staurosporine, which was subsequently also included in the pipette and bath solution. In ATP-depleted cells treated with staurosporine, the presence of 1 mM ATP in the pipette failed to restore the whole-cell current response to hypotonicity. Taken together, these results indicate that a phosphorylation step is involved in the activation of Cl^- channels during cell swelling.

It has previously been reported that in lung cancer cells the lack of ATP not only prevented the activation of a Cl^- conductance upon exposure to extracellular hypotonicity but also prevented hypotonic cell swelling (Jirsch et al., 1994). This is in contrast to our findings in M-1 cells. ATP-depleted M-1 cells had a largely depressed Cl^- current response to hypotonicity but showed a normal degree of hypotonic cell swelling. On average, the diameter of ATP-depleted cells dialyzed with ATP-free pipette solution or with a pipette solution containing 1 mM AMP-PNP increased from 15.6 ± 0.6 to 20.6 ± 0.7 μm (n = 20, $P \leq 0.001$) upon exposure to hypotonic bath solution and returned to 14.9 ± 0.8 μm (n = 14) after washout. These values are in good agreement with those observed in control cells (Table I). Moreover, in ATP-depleted cells in which the Cl^- current response was restored by including ATP or ATPγS in the pipette solution, the cell diameter similarly increased from 17 ± 0.6 to 21.4 ± 0.7 μm (n ± 19, $P \leq 0.001$) upon exposure to hypotonic bath solution and returned to 15 ± 0.7 μm (n = 17) after washout. Thus, our experiments demonstrate that hypotonic cell swelling was independent of intracellular ATP and independent of the presence or absence of a stimulated Cl^- conductance.

Attempts to Resolve Single Channel Currents

We have previously shown that in M-1 cells single-channel current events of nonselective cation channels can be resolved in the whole-cell recording configuration under appropriate conditions (Volk et al., 1995*a*). In an attempt to resolve single-channel Cl^- currents, we used symmetrical NMDG-Cl solutions (125 mM) in the pipette and in the bath to eliminate any cation currents. Furthermore, in these experiments cells were only briefly exposed to a hypotonic bath solution, and we focused our attention on the early phase of $I_{Cl\text{-}swell}$ activation and on the recovery phase of the currents back to baseline current levels after washout of the hypotonic solution. An example of such an experiment is shown in Fig. 8. The holding potential was −60 mV throughout the experiment. Brief exposure of the cell to hypotonic bath solution induced a reversible increase of the whole-cell inward current. During hypotonic activation the whole-cell current trace became rather noisy and flickery. Interestingly, the current increase during hypotonicity and the current decline back to the baseline current level during washout did not occur in a smooth and continuous way but with step-like changes of the whole-cell current level. In this experiment the step-like changes of the whole-cell current were most prominent during the recovery phase from hypotonic activation. A closer analysis of these current steps revealed step amplitudes of 1.8 and 2.4 pA (Fig. 8 *B*). Inspection of the current trace during the final recovery back to the baseline current level demonstrates the presence of even smaller current steps with amplitudes of 1.2 and 0.6 pA. Current steps with similarly spaced amplitudes were also observed at other holding potentials, and examples of current traces recorded at depolarizing voltages are shown in Fig. 9. At any given voltage the larger steps had about 2, 3, or 4 times the amplitude of the smallest current steps observed at that voltage, but not all of the different step amplitudes were detected in each individual experiment. The histogram shown in Fig. 10 *A* summarizes the various current step amplitudes detected in a total number of 17 experiments at a holding potential of −60 mV. Four individual peaks are clearly visible, and the corresponding step amplitudes averaged 0.62 ± 0.01 pA (n = 16), 1.23 ± 0.02 pA (n = 15), 1.79 ± 0.01 pA (n = 14), and 2.37 ± 0.01 pA (n = 11). The equidistant peaks suggest that the larger steps are multiples of the smallest current step detected. If the smallest step corresponds to the single-channel current amplitude of the underlying swelling-activated Cl^- channel, the larger steps may reflect a coordinated gating of several individual channels. Similar analyses were also performed at other pipette potentials, and Fig. 10 *B* summarizes these data. The data points from the smallest detectable whole-cell current steps at each holding potential were used to construct a tentative single channel *I-V* curve ($1 \times i$). This curve indicates that the corresponding single-channel displays outward rectification with slope conductances of 55 pS at +120 mV, 8 pS at −120

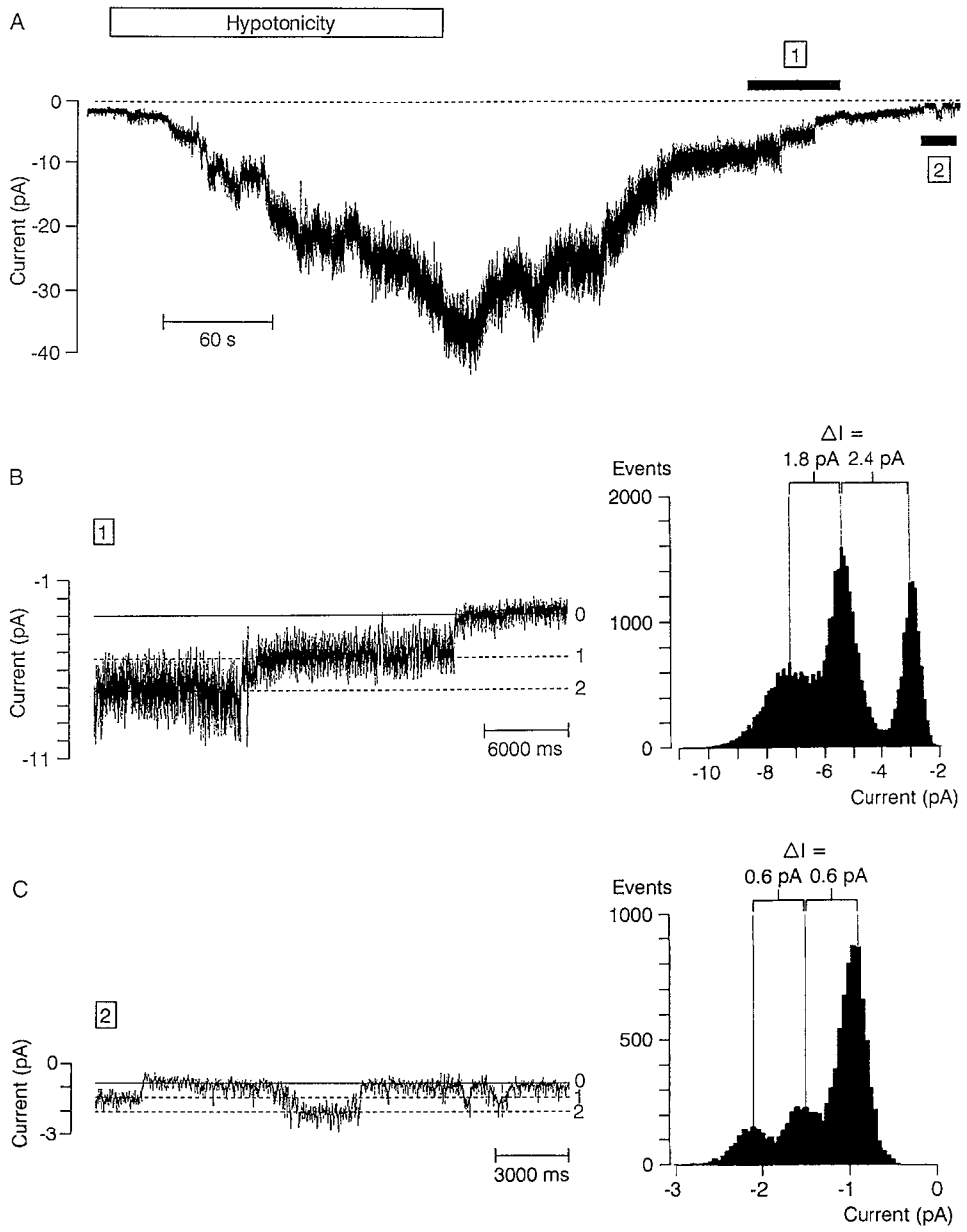

FIGURE 8. High-resolution whole-cell recording of swelling-activated Cl^- current reveals step-like changes of the current level during recovery from hypotonic activation. 125-NMDG-Cl/EGTA pipette solution and 125-NMDG-Cl bath solution were used, and extracellular hypotonicity was achieved by removal of 50 mM sucrose. The continuous whole-cell current trace shown in *A* was recorded at a holding potential of −60 mV and illustrates the current activation during hypotonicity and the subsequent recovery to baseline current level. Two portions of this current trace (indicated by *black bars* and the numbers *1* and *2*) are shown on expanded scales in *B* and *C*. Current amplitude histograms are shown to the right of each trace. The peaks of the histograms were used to estimate the amplitudes ΔI of the current steps. The current signal was filtered at 300 Hz in *A* and *B* and at 100 Hz in *C*.

mV, and 15 pS at 0 mV. The outward to inward current ratio (at +120 mV and −120 mV) of 3.6 is in good agreement with the ratio of 3.5 found for $I_{Cl\text{-}swell}$ in whole-cell current recordings. The three other curves are scaled-up versions of this single channel *I-V* curve using the factors 2, 3, and 4. These theoretical curves ($2 \times i$, $3 \times i$, and $4 \times i$) nicely fit the experimental data points corresponding to the larger size current steps measured at different holding potentials. This is in favor of the interpretation that the larger current steps result from coordinated gating of several single channels.

DISCUSSION

In the present study we have characterized a swelling-activated Cl^- conductance in M-1 CCD cells and have identified the underlying single-channels in whole-cell current recordings. During hypotonic cell swelling the whole-cell Cl^- conductance of M-1 cells reversibly increases by > 30-fold. The most prominent properties of the stimulated Cl^- conductance are an outward rectification, a characteristic depolarization-induced inactivation, and a hyperpolarization-induced activation. As far as we know, swelling activated Cl^- channels have not yet been described in CCD cells in situ. As previously shown, cultured M-1 cells preserve morphological and functional properties typical for CCD principal cells in vivo (Korbmacher et al. 1993). Thus, our findings indicate that swelling-activated Cl^- channels are likely to be present in CCD principal cells. Since the experiments were performed in single M-1 cells which had not yet formed a polarized epithelium, we could not discrimi-

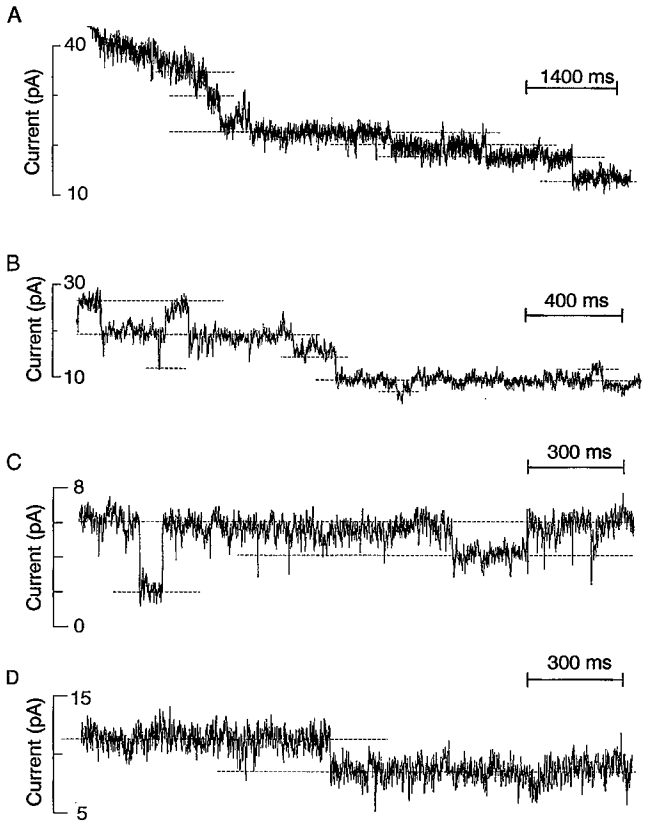

FIGURE 9. Whole-cell current steps at depolarizing potentials. In similar experiments as shown in Fig. 8 the pipette potential was occasionally stepped from a holding potential of −60 mV to depolarizing test potentials during recovery from hypotonic activation. In *A–D* representative whole-cell current traces from four different experiments are shown which were recorded immediately after stepping the pipette potential from −60 to +90 mV (*A, B, and D*) or from −60 to +80 mV (*C*). The amplitudes of step like changes of the whole-cell current level were estimated as indicated by dotted lines. Current signal was filtered at 500 Hz.

nate between apical and basolateral conductance components. Thus, it remains to be determined whether in polarized CCD cells swelling-activated Cl^- channels are expressed apically or basolaterally or in both membranes.

Voltage Dependence of the Swelling-activated Cl^- Conductance

Swelling-activated Cl^- currents have been observed in numerous cell types, and outward rectification and depolarization-induced inactivation seem to be characteristic features of this type of conductance. However, the extent and rate of depolarization-induced inactivation are quite variable from preparation to preparation (for review, see Strange et al. 1996). In rat C6 glioma cells (Jackson and Strange, 1995*a*) the voltage dependence of inactivation has been carefully studied with similar voltage-step protocols as used in the present study in M-1 cells. In C6 cells maximal current inactivation was 87% with an inactivation midpoint at 69 mV and an effective gating charge of 3–4. In M-1 cells the corresponding values were 80%, 73 mV, and 1–2, respectively. Possibly as a result of the smaller gating charge the depolarization-induced current inactivation is not as rapid in M-1 cells as in the C6 cells. Within the first 100 ms of a depolarizing voltage step to +120 mV the outward currents in M-1 cells and C6 cells decayed by ~13 and 32%, respectively. Nevertheless, the overall characteristics of the depolarization-induced current inactivation are qualitatively very similar in both systems. Moreover, in C6 cells and in M-1 cells $I_{Cl\text{-}swell}$, after depolarization-induced inactivation is similarly reactivated by hyperpolarizing potentials, a phenomenon which has also been noticed in intestinal epithelial cells (Kubo and Okada, 1992). In M-1 cells channel reactivation already occurred at a holding potential of −20 mV but was faster at more negative potentials. Hyperpolarization of M-1 cells from a holding potential of −60 to −90 or −120 mV further activated $I_{Cl\text{-}swell}$. This voltage dependence may be physiologically important, since it allows the swelling-activated Cl^- channels to be active at physiological membrane potentials, the negativity of which may regulate overall channel activity. At present we do not know whether cell swelling activates more than one type of Cl^- channel in M-1 cells, and it is conceivable that the voltage dependence of $I_{Cl\text{-}swell}$ is mediated by a subset of swelling-activated Cl^- channels. Interestingly, the hyperpolarization-induced activation and depolarization-induced inactivation of $I_{Cl\text{-}swell}$ in M-1 cells is reminiscent of the voltage dependence described for the CIC-2 channel (Thiemann et al., 1992), a member of the CIC-family of so-called "voltage-gated" Cl^- channels (Pusch and Jentsch, 1994). CIC-2 channels expressed in *Xenopus* oocytes can also be activated by cell swelling (Gründer et al., 1992).

Anion Selectivity of the Swelling-activated Conductance

In most studies of swelling-activated anion currents the reported selectivity sequence was $I^- > Br^- > Cl^-$ and was deduced from reversal potential measurements (Rasola et al., 1992). However, when estimating the ion selectivity of a channel, one has to make a distinction between the permeability sequence obtained from reversal potential measurements and the conductance sequence obtained from current measurements. In M-1 cells the reversal potential measurements during hypotonic activation were in excellent agreement with those measured under similar conditions in HeLa-cells (Diaz et al., 1993), intestinal epithelial cells (Kubo and Okada, 1992), or cardiac myocytes (Vandenberg et al., 1994), and revealed a permeability sequence $SCN^- > I^- > Br^- > Cl^- > >$ gluconate. In contrast, the instantaneous outward current measurements revealed a conductance sequence $I^- \approx Br^- \approx Cl^- > SCN^- > >$ glu-

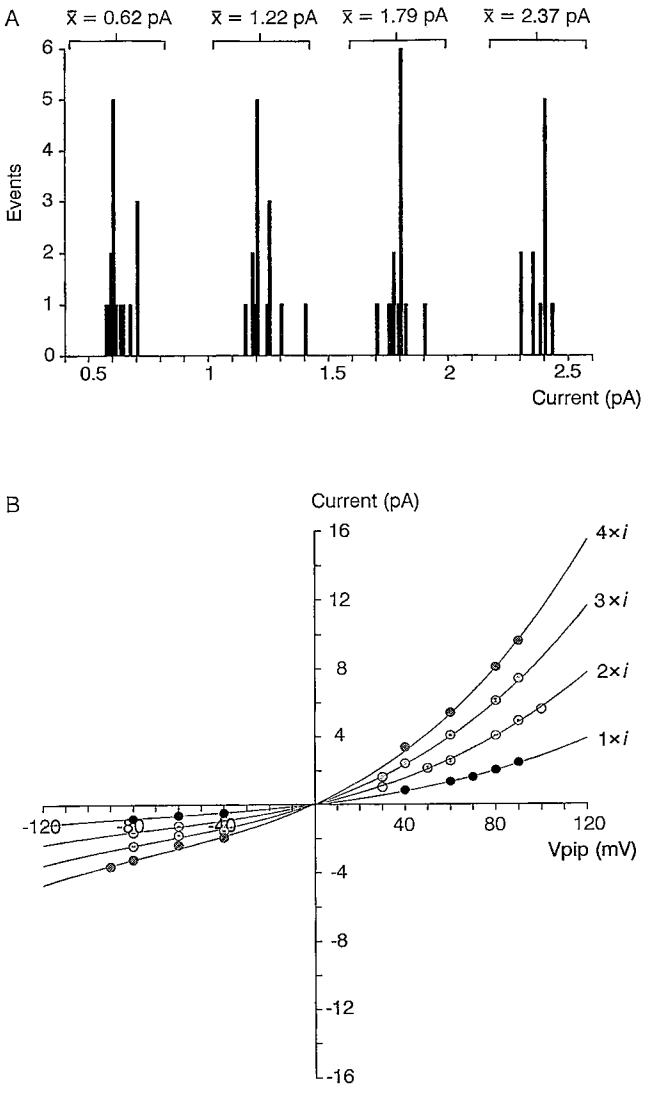

FIGURE 10. Summary of data from 17 experiments. Experimental conditions were the same as described in legend of Fig. 8. The amplitudes of whole-cell current steps during the initial phase of swelling-induced Cl^- current activation or during recovery back to baseline were estimated at various holding potentials as shown in Figs. 8 and 9. (*A*) Histogram of current step amplitudes at a holding potential of −60 mV. Current steps with several different amplitudes could be identified in each of the 17 whole-cell recordings. For every individual experiment current steps with similar amplitudes were averaged, and a mean value of usually 2–5 measurements (range: 1–13) was included in the histogram as one event. Four individual peaks are visible in the histogram. Events were summarized as indicated, and for each group of events the mean current step amplitude was calculated. Similar analyses were also performed at other holding potentials and results are summarized in *B*. The mean current step amplitudes were plotted versus the holding potential (V_{pip}). Each data point represents an average value obtained from 1 to 16 out of the 17 experiments. The smallest detectable whole-cell current steps at each holding potential were used to construct a tentative single channel *I-V* curve ($1 \times i$) which revealed an outward slope conductance of 55 pS at +120 mV, and inward slope conductance of 8 pS at −120 mV, and and a slope conductance of 15 pS at 0 mV. The three other *I-V* curves shown are scaled-up versions of the single-channel *I-V* curve using the factors 2 ($2 \times i$), 3 ($3 \times i$), and 4 ($4 \times i$).

conate. Interestingly, the conductance sequence obtained from nearly steady state current data at the end of 400-ms voltage pulses was again $SCN^- > I^- > Br^- \geq Cl^- > >$ gluconate, which corresponds well with the sequence deduced from the reversal potential measurements. This may be explained by our observation that the kinetics of channel inactivation are altered by the different anions permeating the channel. In the case of SCN^- the rate of channel inactivation during depolarization is significantly reduced compared to channel inactivation in the presence of Cl^-, and at the end of a depolarizing voltage pulse the outward currents carried by SCN^- were larger than the corresponding outward currents carried by Cl^-. Our results suggest that the charge carrying ions are involved in the gating mechanisms of the channel. Interestingly, a mechanism in which gating is intrinsically linked to permeation has recently been suggested for the *Torpedo* Cl^- channel CIC-O. In this channel voltage-dependent gating seems to be conferred by the permeating ion itself, acting as the gating charge (Pusch et al., 1995). However, the Cl^- channels of the CIC-family, including the swelling-activated CIC-2 channel (Thiemann et al., 1992), have typically a selectivity sequence of $Cl^- \geq Br^- > I^-$ (Pusch and Jentsch, 1994) which is not compatible with the selectivity sequence of the endogenously expressed swelling-activated Cl^- conductance found in many cells, including M-1 cells. The selectivity sequence of the endogenous swelling-activated Cl^- conductance is also different from the selectivity sequence $Br^- \geq Cl^- > I^-$ of cAMP-regulated Cl^- conductances in cells expressing wild-type CFTR (Anderson et al., 1991). Such a CFTR-like Cl^- conductance can also be detected in M-1 cells after stimulation with forskolin (Korbmacher and Letz, 1995). The selectivity sequence of the swelling-activated Cl^- conductance is compatible with the sequence $SCN^- > I^- > Br^- > Cl^-$ reported for the Cl^- conductance related to the expression of I_{Cln}, a putative Cl^- channel or channel regulatory protein (Paulmichl et al., 1992; Krapivinsky et al., 1994). It has recently been shown that I_{Cln} antisense oligonucleotides suppress swelling-induced activation of Cl^- channels in NIH 3T3 fibroblasts (Gschwentner et al., 1995*b*).

Pharmacological Characterization of the Swelling-activated Cl^- Conductance

The $I_{Cl\text{-}swell}$ in M-1 cells was effectively inhibited by the "classical" Cl^- channel blockers NPPB and DIDS in similar concentrations as previously used to inhibit $I_{Cl\text{-}swell}$ in other types of cells. NPPB and DIDS have been shown to inhibit an outwardly rectifying Cl^- channel (Hayslett et al., 1987), which is present in many different cells, including M-1 cells (Volk et al., 1995*b*). We have previously shown that the outwardly rectifying Cl^- channel in inside/out patches of M-1 cells is sensitive to

glibenclamide. Interestingly, glibenclamide also inhibits $I_{Cl\text{-}swell}$ in M-1 cells. However, neither the classical blockers, NPPB and DIDS, nor glibenclamide (Rabe et al., 1995) are specific inhibitors. Thus, we cannot deduce from these pharmacological data that the outwardly rectifying Cl^- channel corresponds to the channel activated during cell swelling.

Niflumic acid and flufenamic acid partially inhibit $I_{Cl\text{-}swell}$ in M-1 cells. Niflumic acid, which is known to block calcium-activated Cl^- currents (Pacaud et al., 1989), did not significantly inhibit $I_{Cl\text{-}swell}$ in *Xenopus* oocytes (Ackerman et al., 1994). We could show that $I_{Cl\text{-}swell}$ in M-1 cells is calcium independent, which argues against a specificity of niflumic acid for calcium-activated Cl^- currents. Flufenamic acid has been used as a blocker of nonselective cation channels and has been shown to block effectively nonselective cation channels in M-1 cells (Volk et al., 1995*a*). However, the effect of flufenamic acid on $I_{Cl\text{-}swell}$ demonstrates that this substance is not a specific blocker of nonselective cation channels.

$I_{Cl\text{-}swell}$ was also inhibited by tamoxifen, an antiestrogen, that has recently been shown to block the swelling-activated Cl^- conductance in T84 colonic carcinoma cells, without affecting calcium-activated and cAMP-activated Cl^- conductances, which are also present in these cells (Valverde et al., 1993). In the meantime, tamoxifen has been shown to inhibit the swelling-activated Cl^- conductances in endothelial cells (Nilius et al., 1994*b*), in fibroblasts and lung carcinoma cells (Zhang et al., 1994), and in cardiac myocytes without affecting a cAMP-activated Cl^- conductance (Vandenberg et al., 1994). In these studies the onset of tamoxifen action and the washout of the drug were much slower than the effects of other channel blockers, like DIDS or NPPB, which is in good agreement with our findings in M-1 cells. Tamoxifen also affected channel gating and produced a more rapid depolarization-induced current inactivation, like the other inhibitors which effectively blocked $I_{Cl\text{-}swell}$ in M-1 cells. A similar effect on $I_{Cl\text{-}swell}$ inactivation has previously been described for SITS in intestinal epithelial cells (Kubo and Okada, 1992) and for DIDS in T-lymphocytes (Lewis et al., 1993). In both preparations the rate of depolarization-induced outward current inactivation was increased in the presence of the inhibitors. This phenomenon was particularly striking in the T-lymphocytes in which $I_{Cl\text{-}swell}$ normally shows very little or no depolarization-induced current inactivation.

Like tamoxifen (Zhang et al., 1994; Valverde et al., 1993), verapamil and dideoxyforskolin have been reported to inhibit $I_{Cl\text{-}swell}$ (Diaz et al., 1993), thought to be related to the expression of p-glycoprotein. However, verapamil had only a minor effect on $I_{Cl\text{-}swell}$ in M-1 cells. Several recent studies suggest that there is no correlation between volume-activated Cl^- currents and the expression of p-glycoprotein (Ehring et al., 1994; Rasola et al., 1994).

We also investigated cAMP and the antiviral drug acycloguanosine which have been shown to inhibit Cl^- currents related to the expression of I_{Cln} (Paulmichl et al., 1992; Gschwenter et al., 1995*a*). However, cAMP in a concentration of 1 mM (70% inhibition of the Cl^- current in oocytes expressing I_{Cln}) had no significant effect on $I_{Cl\text{-}swell}$ in M-1 cells, and acycloguanosine had only a small effect. Thus, we have no pharmacological support for the idea, that the swelling-activated channels in M-1 cells may be related to the expression of I_{Cln}.

Mechanism of Activation

Cell diameter measurements indicated that exposure to hypotonic solutions induced significant cell swelling of whole-cell patch clamped M-1 cells and that cell swelling always preceded current activation. There was an average delay of 71-s after switching to the hypoosmotic external solution before $I_{Cl\text{-}swell}$ was observed, which is in the same range as the reported delay in cardiac myocytes (Vandenberg et al., 1994), bovine chromaffin cells (Doroshenko and Neher, 1992), HT_{29} colon carcinoma cells (Greger et al., 1993), and Jurkat T-lymphocytes (Ross et al., 1994). The slow onset of the conductance increase in all these preparations suggests that the mechanism responsible for channel activation is probably complex and may involve a series of successive steps including mechanical transduction via the cytoskeleton.

Under the conditions of conventional whole-cell patch clamp recordings the relatively small intracellular volume is in continuity with a much larger patch pipette volume. Thus, volume regulatory mechanisms may be activated during cell swelling but cannot effectively reduce intracellular osmolarity. It is therefore not surprising that cell swelling and current activation were sustained in the presence of a hypotonic solution and that we were not able to observe regulatory volume changes (for further discussion of this point, see Worrell et al., 1989; Doroshenko and Neher, 1992; Ross et al., 1994). In contrast, under physiological conditions KCl loss via swelling-activated Cl^- and K^+ channels is likely to mediate regulatory volume decrease. At present, we cannot estimate to what extent $I_{Cl\text{-}swell}$ may contribute to regulatory volume decrease in M-1 cells, since we do not have any data on swelling-activated K^+ channels in M-1 cells and do not know the driving forces for Cl^- and K^+ during cell swelling. In human breast cancer cells it has recently been questioned whether swelling-activated Cl^- channels are involved in volume regulation since no appreciable Cl^- loss or regulatory volume decrease was observed after cell swelling (Altenberg et

al., 1994). However, $I_{Cl\text{-}swell}$ observed in these cells was very small (40 pA at −60 mV) compared to the large currents observed in M-1 cells or in HeLa cells (Diaz et al., 1993), which are known to effectively regulate their volume in response to hypotonic swelling (Tivet et al., 1985).

In many cells, including collecting duct cells (Tinel et al., 1994, Fu et al., 1995), hypotonic cell swelling is associated with an increase of the cytosolic Ca^{2+} concentration (for review, see McCarty and O'Neil, 1992). However, in M-1 cells activation of $I_{Cl\text{-}swell}$ did not depend on the presence of extra- or intracellular Ca^{2+}, which is in agreement with a previous report in intestinal epithelial cells (Kubo and Okada, 1992). Moreover, raising the intracellular Ca^{2+} concentration by using a Ca^{2+} ionophore activates a different type of Cl^- conductance in M-1 cells.

The swelling-induced conductance increase may involve activation of channels already present in the plasma membrane or may require the insertion of additional channels into the cell membrane. In HT_{29} colon carcinoma cells, a 23% increase in cell capacitance was observed during hypotonic cell swelling, which activates a Cl^- conductance in these cells (Greger et al., 1993). This was interpreted as evidence for exocytosis of membrane vesicles containing Cl^- channels. In contrast, in T-lymphocytes a careful analysis of the time course of current activation and capacitance changes during cell swelling revealed a temporal separation between these two parameters. In fact, in T-lymphocytes the conductance increase preceded an increase in cell capacitance. It was therefore concluded that the capacitance changes were not related to the activation of ion channels (Ross et al., 1994). In M-1 cells we did not detect a significant increase of cell capacitance during cell swelling (data not shown).

While cell swelling precedes the current increase and apparently triggers channel activation, it is not sufficient to activate $I_{Cl\text{-}swell}$ in the absence of intracellular ATP. The experiments with ATP-depleted M-1 cells demonstrate that the presence of a high-energy γ-phosphate group is required for channel activation and that channel activation most likely involves a Mg^{2+}-dependent phosphorylation reaction. In contrast to our findings in ATP-depleted M-1 cells, it has previously been reported that including nonhydrolyzable ATP analogues in the pipette solution supported volume-activated Cl^- currents at levels similar to those seen for ATP (Gill et al., 1992; Jackson et al., 1994; Oiki et al., 1994; Jackson et al., 1996). At present we have no explanation for these discrepant findings. The inhibitory effect of staurosporine suggests that protein kinase C may be involved in the activation of $I_{Cl\text{-}swell}$ in M-1 cells, but staurosporine also inhibits several other kinases. In intestinal epithelial cells, hypotonic cell swelling has been reported to trigger the phosphorylation of several proteins on tyrosine residues, as well as phosphorylation of MAP kinase (Tilly et al., 1993). Thus, ATP-dependent phosphorylation steps may be involved in channel activation at several levels of a complex signal transduction cascade.

Single-channel Properties of the Swelling-activated Cl^- Channels

Stationary noise analysis studies have suggested that the channel responsible for $I_{Cl\text{-}swell}$ is very small, i.e. ≤ 1–2 pS (Doroshenko and Neher, 1992; Stoddard et al., 1993; Lewis et al., 1993; Nilius et al., 1994*a*). In contrast, single-channel measurements in several epithelial cells (Worrell et al. 1989; Solc and Wine, 1991; Okada et al., 1994), and in osteoclasts (Kelly et al., 1994) have demonstrated the existence of swelling-activated, outwardly rectifying Cl^- channels with a unitary conductance of 20–90 pS at depolarizing voltages. A possible reconciliation of these discrepant findings comes from a recent study which uses stationary noise analysis, nonstationary noise analysis, and single-channel recordings to determine the single-channel conductance of swelling-activated Cl^- channels in C6 cells (Jackson and Strange, 1995*b*). It was concluded that the stationary noise analysis underestimates the unitary conductance because it incorrectly assumes that a graded increase in the macroscopic current is due to a graded increase in the open probability (P_o) of a constant number of independent channels with a fixed unitary current. Instead, swelling-induced channel activation probably involves an abrupt switching of single-channels from an OFF state, where channel open probability is zero, to an ON state, where open probability is near unity. Thus, during cell swelling the whole-cell current increases because the number of active channels in the membrane increases. Once a channel is activated, its open probability remains more or less constant (Jackson and Stange, 1995*b*). Our results in M-1 cells are in favor of such an interpretation. During the early phase of hypotonic activation we noticed step-like increases of the whole-cell current level, and similar steps were also observed during the recovery back to the baseline current level. Such a discontinuous behavior is not compatible with a graded, continuous increase of P_o of a large and constant number of Cl^- channels. Instead, the amplitudes of these step-like changes of the whole-cell current level suggest that each step corresponds to an insertion or abrupt activation of one to four previously silent channels which subsequently remain active with a high open probability. A single-channel *I-V* curve was constructed using the smallest resolvable current transitions detected at various holding potentials. The deduced single-channel conductance and the degree of outward rectification of the channel in M-1 cells are in

good agreement with the values found in the C6 cell using nonstationary noise analysis and single-channel recordings. The larger current transitions with amplitudes that were two, three, or four times the size of the putative single-channel current transitions may indicate that the underlying Cl^- channels are composed of several channel subunits which conduct individually or in a coordinated fashion. Alternatively, individual channels are arranged in the membrane in such a way that a coordinated gating is likely to occur.

We thank Mrs. U. Fink and Mrs. I. Doering-Hirsch for their expert technical assistance. The authors thank Prof. Dr. E. Frömter for helpful discussions.

This work was supported by a grant from the Deutsche Forschungsgemeinschaft (DFG grant Fr 233/9-1).

Original version received 2 January 1996 and accepted version received 17 June 1996.

REFERENCES

Ackerman, M.J., K.D. Wickman, and D.E. Clapham. 1994. Hypotonicity activates a native chloride current in *Xenopus* oocytes. *J. Gen. Physiol.* 103:153–179.

Altenberg, G.A., J.W. Deitmer, D.C. Glass, and L. Reuss. 1994. P-glycoprotein-associated Cl^- currents are activated by cell swelling but do not contribute to cell volume regulation. *Cancer Res.* 54: 618–622.

Anderson, M.P., R.J. Gregory, S. Thompson, D.W. Souza, S. Paul, R.C. Mulligan, A.E. Smith, and M.J. Welsh. 1991. Demonstration that CFTR is a chloride channel by alternation of its anion selectivity. *Science (Wash. DC).* 253:202–204.

Diaz, M., M.A. Valverde, C.F. Higgins, C. Rucareanu, and F.V. Sepúlveda. 1993. Volume-activated chloride channels in HeLa cells are blocked by verapamil and dideoxyforskolin. *Pflügers Archiv.* 422:347–353.

Doroshenko, P., and E. Neher. 1992. Volume-sensitive chloride conductance in bovine chromaffin cell membrane. *J. Physiol. (Camb.).* 449:197–218.

Ehring, G.R., Y.V. Osipchuk, and M.D. Cahalan. 1994. Swelling-activated chloride channels in multidrug-sensitive and -resistant cells. *J. Gen. Physiol.* 104:1129–1161.

Fu, W.-J., M. Kuwahara, and F. Marumo. 1995. Mechanisms of regulatory volume decrease in collecting duct cells. *Jpn. J. Physiol.* 45: 97–109.

Gill, D.R., S.C. Hyde, C.F. Higgins, M.A. Valverde, G.M. Mintenig, and F.V. Sepúlveda. 1992. Separation of drug transport and chloride channel functions of the human multidrug resistance p-glycoprotein. *Cell* 71:23–32.

Greger, R., N. Allert, U. Fröbe, and C. Normann. 1993. Increase in cytosolic Ca^{2+} regulates exocytosis and Cl^- conductance in HT_{29} cells. *Pflügers Archiv.* 424:329–334.

Gründer, S., A. Thiemann, M. Pusch, and T.J. Jentsch. 1992. Regions involved in the opening of CIC-2 chloride channel by voltage and cell volume. *Nature (Lond.).* 360:759–762.

Gschwentner, M., S. Alex, E. Wöll, M. Ritter, U.O. Nagl, A. Schmarda, A. Laich, G.M. Pinggerra, H. Ellemunter, H. Huemer, et al. 1995*a*. Antiviral drugs from the nucleoside analogue family block volume-activated chloride channels. *Mol. Med.* 1:1076–1086.

Gschwentner, M., U.O. Nagl, E. Wöll, A. Schmarda, M. Ritter, and M. Paulmichl. 1995*b*. Antisense oligonucleotides suppress cell-volume-induced activation of chloride channels. *Pflügers Archiv.* 430:464–470.

Hamill, O.P., A. Marty, E. Neher, B. Sakmann, and F.J. Sigworth. 1981. Improved patch clamp techniques for high-resolution current recording from cells and cell-free membrane patches. *Pflügers Archiv.* 391:85–100.

Hayslett, J.P., H. Gögelein, K. Kunzelmann, and R. Greger. 1987. Characteristics of apical chloride channels in human colon cells (HT_{29}). *Pflügers Archiv.* 410:487–494.

Jackson, P.S., K. Churchwell, N. Ballatori, J.L. Boyer, and K. Strange. 1996. Swelling-activated anion conductance in skate hepatocytes: regulation by cell Cl^- and ATP. *Am. J. Physiol.* 270:C57–C66.

Jackson, P.S., R. Morrison, and K. Strange. 1994. The volume-sensitive organic osmolyte-anion channel VSOAC is regulated by nonhydrolytic ATP binding. *Am. J. Physiol* 267:C1203–C1209.

Jackson, P.S., and K. Strange. 1995*a*. Characterization of the voltage-dependent properties of a volume-sensitive anion conductance. *J. Gen. Physiol.* 105:661–677.

Jackson, P.S., and K. Strange. 1995*b*. Single-channel properties of a volume-sensitive anion conductance. Current activation occurs by abrupt switching of closed channels to an open state. *J. Gen. Physiol.* 105:643–660.

Jirsch, J.D., D.W. Loe, S.P. Cole, R.G. Deeley, and D. Fedida. 1994. ATP is not required for anion current activated by cell swelling in multidrug-resistant lung cancer cells. *Am. J. Physiol.* 267:C688–C699.

Kelly, M.E.M., S.J. Dixon, and S.M. Sims. 1994. Outwardly rectifying chloride current in rabbit osteoclasts is activated by hyposmotic stimulation. *J. Physiol. (Camb.).* 475:377–389.

Korbmacher, C., and B. Letz. 1995. Forskolin stimulates apical Cl^- channels but not amiloride sensitive Na^+ channels in M-1 mouse cortical collecting duct cells. *J. Am. Soc. Nephrol.* 6:342. *(Abstr.).*

Korbmacher, C., A.S. Segal, G. Fejes-Tóth, G. Giebisch, and E.L. Boulpaep. 1993. Whole-cell currents in single and confluent M-1 mouse cortical collecting duct cells. *J. Gen. Physiol.* 102:761–793.

Krapivinsky, G.P., M.J. Ackerman, E.A. Gordon, L.D. Krapivinsky, and D.E. Clapham. 1994. Molecular characterization of a swelling-induced chloride conductance regulatory protein, pI_{Clin}. *Cell.* 76:439–448.

Kubo, M., and Y. Okada. 1992. Volume-regulatory Cl^- channel currents in cultured human epithelial cells. *J. Physiol. (Camb.).* 456: 351–371.

Lang, F., M. Ritter, H. Völkl, and D. Häussinger. 1993. Cell volume regulatory mechanisms: an overview. *Adv. Comp. Environ. Physiol.* 14:1–31.

Letz, B., A. Ackermann, C.M. Canessa, B.C. Rossier, and C. Korbmacher. 1995. Amiloride-sensitive sodium channels in confluent M-1 mouse cortical collecting duct cells. *J. Membr. Biol.* 148:127–141.

Lewis, R.S., P.E. Ross, and M.D. Cahalan. 1993. Chloride channels activated by osmotic stress in T lymphocytes. *J. Gen. Physiol.* 101: 801–826.

McCarty, N.A., and R.G. O'Neil. 1992. Calcium signaling in cell volume regulation. *Physiol. Rev.* 72:1037–1061.

Montrose-Rafizadeh, C., and W.B. Guggino. 1990. Cell volume reg-

ulation in the nephron. *Annu. Rev. Physiol.* 52:761–772.

Nilius, B., M. Oike, I. Zahradnik, and G. Droogmans. 1994*a*. Activation of a Cl^- current by hypotonic volume increase in human endothelial cells. *J. Gen. Physiol.* 103:787–805.

Nilius, B., J. Sehrer, and G. Droogmans. 1994*b*. Permeation properties and modulation of volume-activated Cl^- currents in human endothelial cells. *Br. J. Pharmacol.* 112:1049–1056.

Oike, M., G. Droogmans, and B. Nilius. 1994. The volume-activated chloride current in human endothelial cells depends on intracellular ATP. *Pflügers Archiv.* 427:184–186.

Oiki, S., M. Kubo, and Y. Okada. 1994. Mg^{2+} and ATP-dependence of volume-sensitive Cl^- channels in human epithelial cells. *Jpn. J. Physiol.* 44(Suppl. 2):S77–S79.

Okada, Y., C.C.H. Petersen, M. Kubo, S. Morishima, and M. Tominaga. 1994. Osmotic swelling activates intermediate-conductance Cl^- channels in human interstinal epithelial cells. *Jpn. J. Physiol.* 44:403–409.

Pacaud, P., G. Loirand, J.L. Lavie, C. Mironneau, and J. Mironneau. 1989. Calcium-activated chloride current in rat vascular smooth muscle cells in short-term primary culture. *Pflügers Archiv.* 413: 629–636.

Paulmichl, M., Y. Li, K. Wickman, M. Ackerman, E. Peralta, D. Clapham. 1992. New mammalian chloride channel identified by expression cloning. *Nature (Lond.).* 356:238–241.

Pusch, M., and T.J. Jentsch. 1994. Molecular physiology of voltage-gated chloride channels. *Physiol. Rev.* 74:813–827.

Pusch, M., U. Ludewig, A. Rehfeldt, and T.J. Jentsch. 1995. Gating of the voltage-dependent chloride channel ClC-O by the permeant anion. *Nature (Lond.).* 373:527–531.

Rabe, A., J. Disser, and E. Frömter. 1995. Cl^- channel inhibition by glibenclamide is not specific for the CFTR-type Cl^- channel. *Pflügers Archiv.* 429:659–662.

Rasola, A., L.J.V. Galietta, D.C. Gruenert, and G. Romeo. 1992. Ionic selectivity of volume-sensitive currents in human epithelial cells. *Biochim. Biophys. Acta.* 1139:319–323.

Rasola, A., L.J.V. Galietta, D.C. Gruenert, and G. Romeo. 1994. Volume-sensitive chloride currents in four epithelial cell lines are not directly correlated to the expression of the MDR-1 gene. *J. Biol. Chem.* 269:1432–1436.

Ross, P.E., S.S. Garber, and M.D. Cahalan. 1994. Membrane chloride conductance and capacitance in Jurkat T lymphocytes during osmotic swelling. *Biophys. J.* 66:169–178.

Sheppard, D.N., and M.J. Welsh. 1992. Effect of ATP-sensitive K^+ channel regulators on cystic fibrosis transmembrane conductance regulator chloride current. *J. Gen. Physiol.* 100:573–591.

Solc, C.K., and J.J. Wine. 1991. Swelling-induced and depolarization-induced Cl^- channels in normal and cystic fibrosis epithelial cells. *Am. J. Physiol.* 261:C658–C674.

Stoddard, J., J.H. Steinbach, and L. Simchowitz. 1993. Whole cell Cl^- currents in human neutrophils induced by cell swelling. *Am. J. Physiol.* 265:C156–C165.

Stoos, B.A., A. Náray-Fejes-Tóth, O.A. Carretero, S. Ito, and G. Fejes-Tóth. 1991. Characterization of a mouse cortical collecting duct cell line. *Kidney Int.* 39:1168–1175.

Strange, K., F. Emma, and P.S. Jackson. 1996. Cellular and molecular physiology of volume-sensitive anion channels. *Am. J. Physiol.* 270:C711–C730.

Thiemann, A., S. Gründer, M. Pusch, and T.J. Jentsch. 1992. A chloride channel widely expressed in epithelial and non-epithelial cells. *Nature (Lond.).* 356:57–60.

Tilly, B.C., N. van den Berghe, L.G.J. Tertoolen, M.J. Edixhoven, and H.R. de Jonge. 1993. Protein tyrosine phosphorylation is involved in osmoregulation of ionic conductances. *J. Biol. Chem.* 268:19919–19922.

Tinel, H., F. Wehner, and H. Sauer. 1994. Intracellular Ca^{2+} release and Ca^{2+} influx during regulatory volume decrease in IMCD cells. *Am. J. Physiol.* 267:F130–F138.

Tivet, D.R., N.L. Simmons, and J.F. Aiton. 1985. Role of passive potassium fluxes in cell volume regulation in cultured HeLa cells. *J. Membr. Biol.* 87:93–105.

Valverde, M.A., M. Mintenig, and F.V. Sepúlveda. 1993. Differential effects of tamoxifen and I^- on three distinguishable chloride currents activated in T84 intestinal cells. *Pflügers Archiv.* 425:522–554.

Vandenberg, J.I., A. Yoshida, K. Kirk, and T. Powell. 1994. Swelling-activated and isoprenaline-activated chloride currents in guinea pig cardiac myocytes have distinct electrophysiology and pharmacology. *J. Gen. Physiol.* 104:997–1017.

Volk, T., E. Frömter, and C. Korbmacher. 1995*a*. Hypertonicity activates nonselective cation channels in mouse cortical collecting duct cells. *Proc. Natl. Acad. Sci. USA.* 92:8478–8482.

Volk, T., A. Rabe, and C. Korbmacher. 1995*b*. Glibenclamide inhibits an outwardly rectifying chloride channel in M-1 mouse cortical collecting duct cells. *Cell Physiol. Biochem.* 5:222–231.

Wangemann, P., M. Wittner, A. Di Stefano, H.C. Englert, H.J. Lang, E. Schlatter, and R. Gerger. 1986. Cl^--channel blockers in the thick ascending limb of the loop of Henle: structure activity relationship. *Pflügers Archiv.* 407(Suppl. 2):S128–141.

Worrell, R.T., A.G. Butt, W.H. Cliff, and R.A. Frizzell. 1989. A volume-sensitive chloride conductance in human colonic cell line T84. *Am. J. Physiol.* 256:C1111–C1119.

Zhang, J.J., T.J.C. Jacob, M.A. Valverde, S.P. Hardy, G.M. Mintenig, F.V. Sepúlveda, D.R. Gill, S.C. Hyde, A.E.O. Trezise, and C.F. Higgins. 1994. Tamoxifen blocks chloride channels. *J. Clin. Invest.* 94:1690–1697.